

Streak Camera Performance with Large- Format CCD Readout

*R.A. Lerche, D.S. Andrews, P.M. Bell, R.L. Griffith,
J.W. McDonald, P. Torres III, and G. Vergel de Dios*

This article was submitted to the SPIE Conference, High Speed
and Ultra High Speed Photography, Photonics, and
Videography, San Diego, California, August 3-8, 2003

July 8, 2003

U.S. Department of Energy

Lawrence
Livermore
National
Laboratory

DISCLAIMER

This document was prepared as an account of work sponsored by an agency of the United States Government. Neither the United States Government nor the University of California nor any of their employees, makes any warranty, express or implied, or assumes any legal liability or responsibility for the accuracy, completeness, or usefulness of any information, apparatus, product, or process disclosed, or represents that its use would not infringe privately owned rights. Reference herein to any specific commercial product, process, or service by trade name, trademark, manufacturer, or otherwise, does not necessarily constitute or imply its endorsement, recommendation, or favoring by the United States Government or the University of California. The views and opinions of authors expressed herein do not necessarily state or reflect those of the United States Government or the University of California, and shall not be used for advertising or product endorsement purposes.

This is a preprint of a paper intended for publication in a journal or proceedings. Since changes may be made before publication, this preprint is made available with the understanding that it will not be cited or reproduced without the permission of the author.

STREAK CAMERA PERFORMANCE WITH LARGE-FORMAT CCD READOUT

R. A. Lerche, D. S. Andrews, P. M. Bell, R. L. Griffith,
J. W. McDonald, P. Torres III, G. Vergel de Dios

Lawrence Livermore National Laboratory, 7000 East Avenue, Livermore, CA 94551

ABSTRACT

The ICF program at Livermore has a large inventory of optical streak cameras that were built in the 1970s and 1980s. The cameras include micro-channel plate image-intensifier tubes (IIT) that provide signal amplification and early lens-coupled CCD readouts. Today, these cameras are still very functional, but some replacement parts such as the original streak tube, CCD, and IIT are scarce and obsolete. This article describes recent efforts to improve the performance of these cameras using today's advanced CCD readout technologies. Very sensitive, large-format CCD arrays with efficient fiber-optic input faceplates are now available for direct coupling with the streak tube. Measurements of camera performance characteristics including linearity, spatial and temporal resolution, line-spread function, contrast transfer ratio (CTR), and dynamic range have been made for several different camera configurations: CCD coupled directly to the streak tube, CCD directly coupled to the IIT, and the original configuration with a smaller CCD lens coupled to the IIT output. Spatial resolution (limiting visual) with and without the IIT is 8 and 20 lp/mm, respectively, for photocathode current density up to 25% of the Child-Langmuir (C-L) space-charge limit. Temporal resolution (fwhm) deteriorates by about 20% when the cathode current density reaches 10% of the C-L space charge limit. Streak tube operation with large average tube current was observed by illuminating the entire slit region through a Ronchi ruling and measuring the CTR. Sensitivity (CCD electrons per streak tube photoelectron) for the various configurations ranged from 7.5 to 2,700 with read noise of 7.5 to 10.5 electrons. Optimum spatial resolution is achieved when the IIT is removed. Maximum dynamic range requires a configuration where a single photoelectron from the photocathode produces a signal that is 3 to 5 times the read noise.

1. INTRODUCTION

The Lawrence Livermore National Laboratory (LLNL) Laser Programs built more than 30 of its a high-speed optical streak cameras¹ in the 1970s and 1980s. These cameras have provided the Inertial Confinement Fusion (ICF) Program with high-speed recording capability for nearly 30 years. The cameras are used as the recording device for a variety of laser², x-ray³, and particle instruments⁴ used in experiments that require temporal resolutions approaching 10 picoseconds. The cameras use a large format (40-mm) RCA C73435 streak tube directly coupled to a microchannel-plate image-intensifier tube (MCP IIT). Before 1987, images were captured on hard-film at the output of the IIT. In the mid 1980s, 15 cameras were built for the Nova laser project. These incorporated CCD readouts in place of the earlier film packs. Coupling between the IIT and the CCD was done with a lens system with a reduction ratio of $\sim 2.5:1$ because direct fiber-optic coupling was not yet reliable.

While the original optical streak cameras have worked extremely well for the ICF Program, they are becoming difficult to maintain. The streak tube, the IIT, and several other components are no longer commercially available. The projected need of approximately 50 optical streak cameras for the National Ignition Facility (NIF) will require identification of replacement parts for existing cameras and the acquisition of additional cameras. The work reported in this article is related to LLNL's program for upgrading the current optical streak cameras using the most recent CCD technology. By using a large format CCD directly coupled to the output of the streak tube, it is possible to eliminate the IIT and the lens coupling. It has long been known, that the MCP IIT degrades spatial performance of the streak camera⁵, thus its elimination could also result in improved spatial resolution.

In this paper we report the performance of the RCA C73435 based streak camera using three readout configurations:

1. Streak tube directly coupled to large-format CCD readout,
2. Streak tube and MCP IIT directly couple to large format at CCD readout,
3. Streak tube and MCP IIT lens couple to smaller CCD readout (original design).

This article begins with a description of the three streak camera configurations studied, followed by descriptions of the characterization parameters and techniques used, and comments that differentiate the characterization process from the calibration process. For a direct comparison of the camera performance using these three different configurations, the reader is directed to the table of results in the discussion section at the end of this paper.

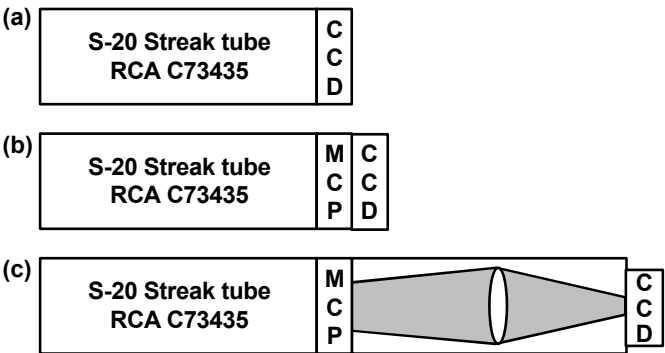
2. CAMERA CONFIGURATIONS

The streak camera configurations characterized in this work are all based on the RCA C73435 streak tube. The basic “blue box” camera (named for its LLNL “laser blue” color) was developed during the 1970s. It included a 40-mm, proximity focused IIT F4113 MCP IIT directly coupled to the streak tube for signal amplification, and used contact film for recording the output image. Circuit improvements and CCD readout were added in the 1980s. The original CCD readout was a Photometrics camera incorporating a Thompson 5881 CCD, a 576 X 384 array of 24-μm square pixels. The CCD was lens coupled to the IIT with an image-size reduction of approximately 2.5:1. In 1996, the ICF Program began replacing these obsolete CCD readouts with Photometrics SenSys 1600 cameras containing Kodak KAF 1600 CCDs that have 1534 x 1024 arrays of 9-μm pixels. The Kodak CCD has properties very similar to the original Thompson CCD. It is exactly the same size as the original, its sensitivity of 20 e-/ADU is similar to the original 25 e-/ADU, and with 3x3 binning the 27 μm pixels are close to the original 24 μm. The newer readout uses the same lens coupling design as the earlier CCD.

Detailed characterization of the camera done in the late 1980s established optimum operating parameters that are still used today. Two of the most significant operating parameters are the MCP IIT gain⁶ and the input slit configuration⁷. The IIT luminous gain is routinely set at 4,000. At this gain, signal from a single photoelectron is well matched to the noise characteristics of the streak camera to provide maximum dynamic range. The standard streak camera input consists of an external slit whose image is optically relayed to the photocathode of the streak tube. Originally, the slit width was set at 100 μm. During characterization work, it was discovered that the parallel wire structure of the extraction grid in the streak tube allowed electrostatic focusing of a wide input slit down to a fine output line comparable to the output achieved with a 100-μm wide slit. Standard camera setup includes setting the input slit width to 1000 μm. This provides the camera with two advantages: A factor of 10 increase in useful photocathode area and thus a factor of 10 increase in sensitivity to low-level signals, and the photocathode current density is reduced by a factor of 10 to achieve the same amplitude output signal.

The main goal of this work was to evaluate performance of the streak tube directly coupled to a large-format CCD array. The CCD chosen to this work is an SI S-800 CCD containing a 4,096 X 4,096 array of 9 μm pixels. If successful, the system could be operated without an MCP IIT and possibly provide improved spatial resolution. Three different streak camera configurations were used for the work reported in this article (see Fig. 1).

- 1 Streak tube directly coupled to large-format CCD readout,
- 2 Streak tube, MCP IIT directly couple to large format at CCD readout,
- 3 Streak tube, MCP IIT lens couple to smaller CCD readout (original design).



3. STREAK CAMERA CHARACTERIZATION AND CALIBRATION

Streak camera characterization is the process of evaluating a set of performance parameters that give a detailed understanding of how well a particular camera configuration performs under a variety of operating conditions. Characterization is done to determine the optimum configuration of a camera and the best component settings. Full

characterization is typically done for only a couple of cameras of any particular design. Characterization tests for the optical cameras evaluated in this study fall into six main categories:

1. Streak tube sensitivity and current limit,
2. Background measurements,
3. System sensitivity measurements,
4. Spatial resolution,
5. Temporal resolution, and
6. Dynamic range.

Once the basic performance of a camera configuration is understood, full characterization of additional cameras with that configuration is not usually needed. Instead, each additional camera requires careful calibrations that allow recorded images to be corrected for camera-to-camera component variations. Typical camera calibrations are:

1. Streak tube sensitivity measurement
2. Temporal response check – Static linewidth,
3. Spatial resolution check - line-spread function,
4. Time base calibration – for non-uniform sweep rates,
5. Flat field – for non-uniform gain response,
6. Geometrical distortion, and
7. Sweep plate to extraction grid tilt.

3.1 Streak tube sensitivity and current limit

Measurement of the streak tube sensitivity and a calculation of its Child-Langmuir (C-L) space-charge-limited current are excellent starting points for streak camera characterization. These are two fundamental characteristics that are related only to the streak tube and that ultimately determine streak camera performance limits.

Sensitivity, which is typically measured in units of amps/watt as a function of wavelength, relates photocathode current to the optical power incident on the photocathode. A calibrated DC light source is used to measure sensitivity. The light source illuminates the streak tube through a set of narrow-band filters at various wavelengths and the corresponding photocathode current is measured. Streak tube electrodes (the grids, deflection plates, and anode) are electrically connected together and biased at +300 volts relative to the photocathode to collect all photoelectrons emitted from the photocathode. Since streak cameras are used to observe relatively short duration pulses of light, sensitivity is often thought of in units of Coulombs/Joule. Typical sensitivities for the RCA C73435 with S-1 and S-20 photocathodes at typical ICF laser wavelengths are listed in Table 1.

The maximum useful tube current (or maximum useful charge in a short pulse) is proportional to the C-L space-charge-limited current. This quantity depends on the internal geometry of the streak tube and the bias potentials applied to the electrodes. For the RCA tube, the photocathode and extraction grid closely approximate a parallel plate photodiode and determine the C-L limited current (see Fig. 2). The C-L current in this configuration is given by:

$$J_0 = (4\epsilon_0/9)(2e/m)^{1/2}(V^{3/2}/x^2),$$

where J_0 is the C-L space-charge-limited current density (amps/cm²), ϵ_0 is the emissivity in vacuum ($1/36\pi \times 10^9$ C), e is the charge of an electron, m is the mass of an electron, x is the electrode separation, and V is the potential between photocathode and extraction grid. For the RCA C73435, x and V are 7 mm and 2500 volts, respectively. Because the extraction grid is formed by a set of parallel wires 5 mm apart rather than a tight mesh used in many other streak tubes, the electric field at the photocathode is reduced slightly below that of two parallel grids. The C-L limit at 2,500 and 2,000 volts respectively is 0.59 and 0.43 Amps/cm². Thus, this streak tube is expected to have a C-L space-charge-limited current of around 0.5 Amps/cm². The laser power density required to reach this current is given by:

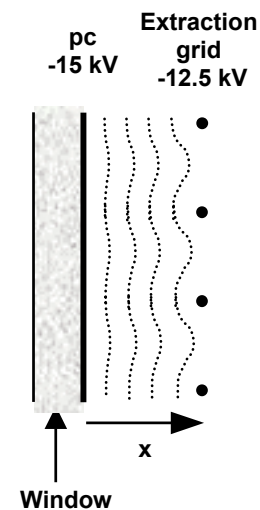


Table 1. Typical streak tube sensitivities, and power density and pulse energy needed to reach C-L space-charge-limited current. ($V = 2 \text{ kV}$, $\Delta t = 100 \text{ ps}$, $A = 0.03 \text{ cm}^2$)				
Photocathode	Wavelength	S (mA/W)	P_{j0} (W/cm ²)	E_{j0} (pJ)
S-1	1.06 μm	0.4	1,064	3,189
	0.53 μm	0.8	503	1,509
	0.35 μm	4.5	94	282
S-20	0.53 μm	50.0	8	24
	0.35 μm	40.0	11	33

$$P_{j0} = J_0/S,$$

where S is the photocathode sensitivity. The required laser energy needed to reach the C-L current limit is

$$E_{j0} = J_0 \Delta t A/S,$$

where Δt is the pulse length, and A is the illuminated area of the photocathode. Table 1 lists the power density P_{j0} and pulse energy E_{j0} needed to reach the C-L space-charge-limited current at typical 1ω , 2ω , and 3ω laser wavelengths. Note the small amount of energy needed to reach the C-L current limit. Typically, a tenth of the C-L limit (a few pJ into an S-20 photocathode) will cause noticeable saturation effects in the tube. (See Ref. 8 for a more thorough discussion of the C-L current.)

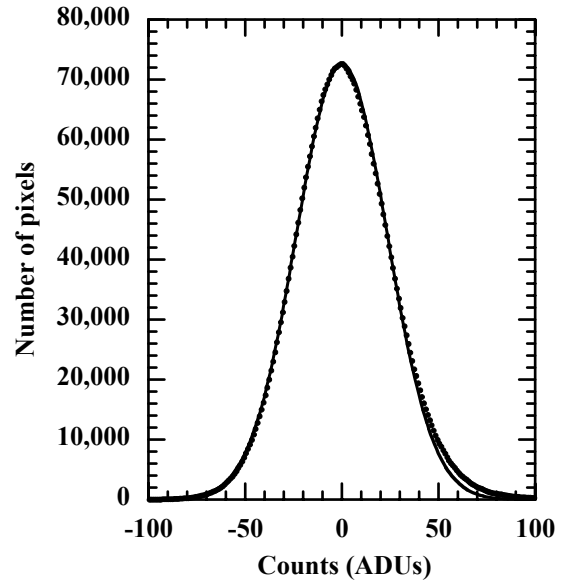
3.2 Background Measurements

Background images provide estimates for three basic system performance characteristics: read noise, dark current noise, and signal threshold. The CCD readout is delivered with a specification sheet that lists its read noise and dark current noise for its various gain settings. Background images allow us to verify these measurements and determine any additional noise introduced by other streak camera components. The standard deviation of the measured background σ_{meas} is the quadrature sum of the dark current noise σ_{dark} and the read noise σ_{read} . Because the dark current noise is proportional to image area and the read noise is independent of image area, background measurements made with different binning configurations can be used to determine the read noise and dark current noise. For example, if 2x2 and 3x3 pixel binning are considered, then the following set of three equations with three unknowns can be written:

$$\begin{aligned}\sigma_{\text{meas } 2 \times 2}^2 &= \sigma_{\text{dark } 2 \times 2}^2 + \sigma_{\text{read}}^2 \\ \sigma_{\text{meas } 3 \times 3}^2 &= \sigma_{\text{dark } 3 \times 3}^2 + \sigma_{\text{read}}^2 \\ \sigma_{\text{dark } 2 \times 2}^2 &= (4/9)\sigma_{\text{dark } 3 \times 3}^2\end{aligned}$$

Thus, simply measuring the standard deviation of background images recorded with 2x2 and 3x3 binning allows calculation of dark current and read noise.

Some care must be taken in interpreting background images. Often, a background image will have a noticeable tilt because the last pixel read accumulates significantly more dark current than the first pixel read. The tilt adds to the standard deviation in the background image. There are several ways to handle the effect of the tilt. For this work, background images were recorded and smoothed with a large (11x11) boxcar filter. The raw image minus the filtered image forms a difference image containing only the noise centered at 0. This is shown in the histogram for the difference image presented in Fig. 3. Dark current noise and



read noise measured for the two configurations with the large format CCD show that virtually all of the noise comes from the CCD and a negligible amount comes from the streak tube and MCP IIT. Measured read noise of 8.52 and 10.96 e^- at CCD gains of 0.43 and 2.31 e^-/ADU match the manufacturers measurements of 7.67 and 10.34 e^- , respectively. Dark current noise is independent of gain. For 2-second exposures, dark current noise in 2x2 bins was 5.67 and 5.80 e^- .

Streak camera image noise determines the smallest signal or threshold that can be detected, and thus sets a lower limit for the camera's dynamic range. Different groups and manufacturers use somewhat different criteria for this value ranging from σ_{meas} to $5\sigma_{\text{meas}}$. For this article we use the conservative value of $5\sigma_{\text{meas}}$.

3.3 System Sensitivity Measurements

Full streak camera system sensitivity measurements are important for understanding dynamic range. In section 3.1 we discussed the relationship between incident optical energy and streak tube current. To fully understand a streak camera, it is necessary to relate streak tube current to the observed output signal intensity. Full system sensitivity can be expressed in several different ways: ADUs/ pe^- , CCD e^-/pe^- , ADUs/nJ, and CCD e^-/nJ . System sensitivity for this work is measured by illuminating a 3-mm by 0.5 mm region of the photocathode with a 15-ns long, square pulse of known energy and recording an image. The number of ADUs in the recorded signal divided by the incident energy generating the signal gives the ADUs/nJ. Using the photocathode sensitivity (Amps/Watt) and the CCD gain (ADUs/CCD e^-) allows conversion of this value to other units. Table 2 contains a summary of the system sensitivities for the three configurations examined for this article.

Table 2. Streak camera system sensitivity for three different camera configurations			
Configuration	SI-800	MCP IIT SI-800	MCP IIT SenSys 1600
ADUs/ pe^-	17.64	1193	25
CCD e^-/pe^-	7.59	2,791	625
ADUs/nJ	2.2×10^9	1.49×10^{11}	3.12×10^9
CCD e^-/nJ	9.4×10^8	3.49×10^{11}	7.81×10^{10}

3.4 Spatial resolution

Two common ways of portraying spatial resolution are the line-spread function (LSF) and the contrast transfer function (CTF). In this work, spatial resolution is initially characterized with a LSF measurement. From the LSF, the CTF is calculated. Then to test the validity of the CTF calculation, the CTF is measured using a Ronchi Ruling mask at appropriate spatial frequencies (typically 4 and 10 lp/mm).

Spatial resolution is referred to the streak tube photocathode. We begin spatial resolution measurements with a determination of the system spatial magnification between the streak tube photocathode and the CCD read out. This is done by illuminating a mask of ten parallel 10- μm wide slits spaced 1.5 mm apart along the streak camera photocathode. For the directly coupled configurations we find the RCA C73435 tube has a spatial magnification of 1.45.

Next, we illuminate a single 10- μm wide spatial slit with a 15-ns long laser pulse. The measured LSF is simply the spatial plot of signal amplitude versus position. Typically, the LSF is measured at a variety of signal amplitudes. For the RCA C73435 without an IIT, measured LSFs had peak amplitudes ranging from 1200 to 32,000 ADUs. A sample image is shown in Fig. 4a and the normalized signals are overlaid in Fig. 4b. For this particular configuration, the shape of the LSF is independent of signal amplitude (that is, no saturation effects are noticed). The LSF has a central spike 50 μm wide (referred to the photocathode). Its peak is 1.5 orders of magnitude above the breakout of the lower level wings. Statistical noise in the wings for the lower level signals is easily noticed.

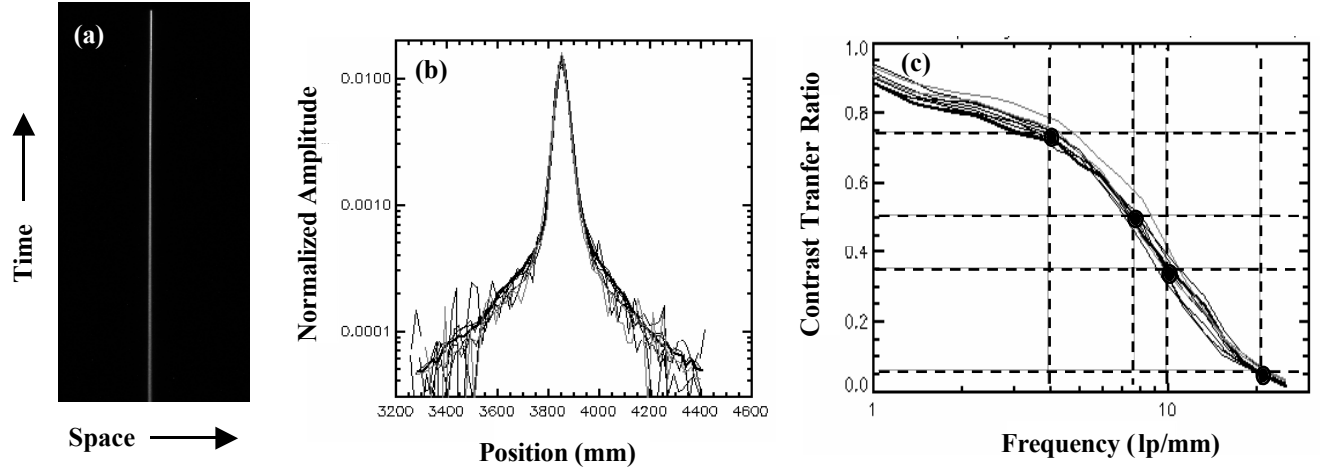


Figure 4. LSF for streak camera configured without IIT. (a) Example of a LSF raw image. (b) Normalized LSF for signals with amplitudes ranging between 1200 and 32,000 ADUs, and (c) CTF calculated from LSF in (b).

A set of convolution calculations transforms the LSF into a contrast transfer function (CTF). Square wave masks at various frequencies (lp/mm) are simply convolved with the LSF to estimate the contrast transfer ratio (CTR). The LSFs in figure 4b are plotted as CTFs in figure 4c. The low level wing of the LSF causes the roll-off of the CTF between 1 and 4 lp/mm. The CTF and LSF are two different but equivalent ways to express system spatial resolution. Other popular ways of expressing resolution such as fwhm, CTR at 50% contrast or CTR at 5% (limiting visual) tell only part of the story.

CTR measurements are performed at 4 and 10 lp/mm to confirm the validity of the CTF curve calculated from the LSF see Fig. 5). Measurements are made using a Ronchi ruling placed along the streak camera slit and illuminated by a collimated laser beam. Analysis consists of first determining envelope functions for the peaks (Max(x)) and the valleys (Min(x)) of the spatial lineout. Then the CTR is calculated from these curves as:

$$CTR(x) = [Max(x) - Min(x)] / [Max(x) + Min(x)]$$

This technique allows calculation of the CTR without requiring spatially uniform illumination of the input slit.

Ronchi ruling measurements allow high current operation of the tube to be characterized (see Fig. 6). By making measurements with varying intensity input signals, the camera response can be characterized as a function of tube current. For low currents the camera remains linear and the CTR observed matches the CTR calculated from the LSF. As input signal intensity increases, streak camera components eventually saturate and go nonlinear causing a loss in spatial

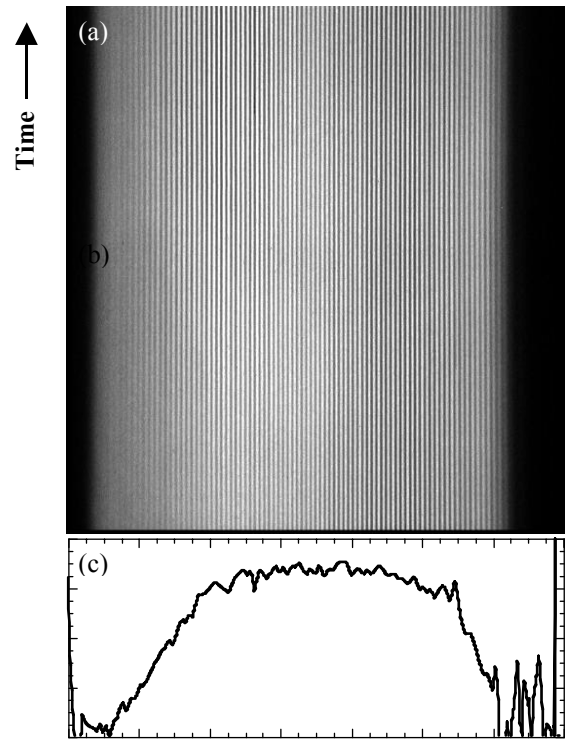
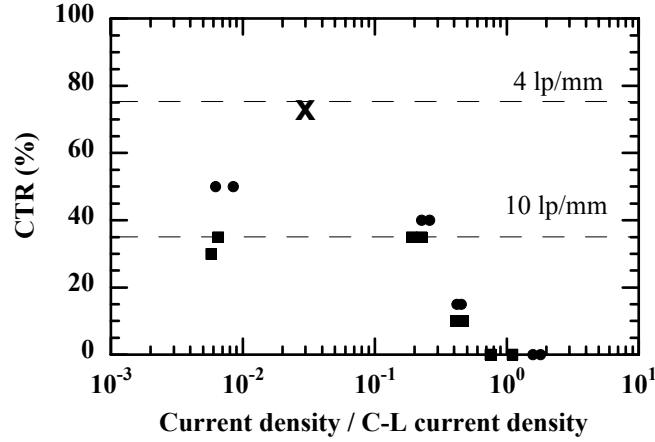


Figure 5. Ronchi ruling CTR measurement. (a) Raw image of 4 lp/mm Ronchi ruling, (b) Spatial intensity profile of (a), (c) CTR calculated from intensity profile in (b).

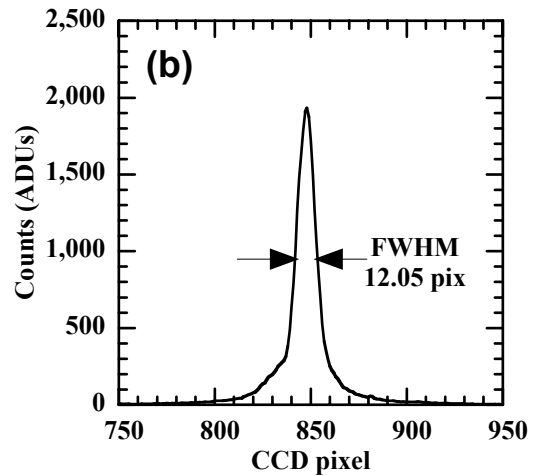
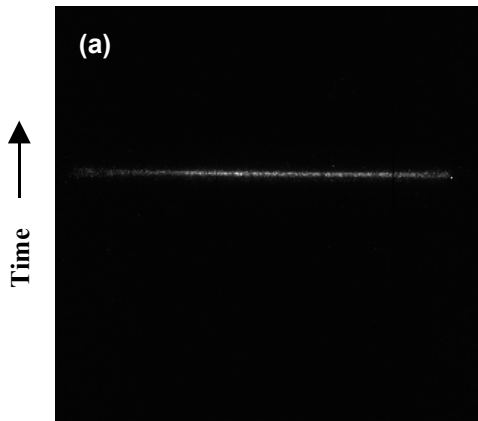


resolution. In the case of the configuration without a MCP IIT, spatial resolution rapidly deteriorates around 30% of C-L space-charge-limited current. Resolution loss caused by the excessive signal current is shown in Fig. 6 where the CTR drops to zero. For average signal amplitudes below 5,000 ADUs (or $0.2J_0$), the CTR matches the values calculated from the LSF. By 10,000 ADU's ($0.4J_0$), a severe decrease in CTR has occurred. For the configuration with no MCP IIT, spatial resolution deteriorates rapidly for tube currents above 25% of C-L.

3.5 Temporal Resolution

A simple static test provides an excellent estimate for a streak camera's temporal resolution. For this measurement, the deflection plates are grounded and the tube illuminated with either a laser pulse or a DC light source to produce a non-swept line image like the one in Fig. 7. The fwhm Δx of the static line represents the best temporal resolution (in pixels) possible with the camera. To form a good estimate for streak camera temporal resolution Δt_{sc} , simply multiply Δx by the dwell time D (ps/pix) of the sweep and add the result in quadrature with the transient time spread of the photoelectrons traveling through the tube:

$$\Delta t_{sc} = [(\Delta x * D)^2 + (\Delta t_{tr})^2]^{1/2}$$



Most of the transient time dispersion is caused by variations in initial electron velocities near the photocathode. For the RCA C73435, Δt_{tr} ranges from 7 to 10 ps depending on photocathode type and wavelength of the light.

Temporal resolution was then checked with a 44 ps laser pulse recorded at three different sweep speeds: a fast sweep, an intermediate sweep, and a slow sweep. At all three sweep speeds, the measured time resolution matches the calculated resolution based on the static line width. In table 3, the measured temporal width matches the estimated response at all sweep speeds. Estimated signal is given by:

$$\Delta t_{est} = [(\Delta t_{sc})^2 + (\Delta t_{laser})^2]^{1/2}$$

The measured signal width is dominated by the laser pulse width at fast sweep speeds; at slow sweeps, the measured signal width is limited by the static line width. The estimated and measured time responses to a 44 ps wide laser pulse show good agreement indicating a good estimate for the camera temporal resolution.

Table 3. Summary of temporal response measurements. Δx = measured static line width, sweep card indicates time window (i.e. 3x is 3 ns window), D is dwell time for sweep card, Δt_{sc} = streak camera resolution estimated from Δx , Δt_{est} = calculated response to a 44 ps laser pulse, Δt_{meas} = measured response to 44 ps laser pulse.					
Δx (pix)	Sweep Card	D (ps/pix)	Δt_{sc} (ps)	Δt_{est} (ps)	Δt_{meas} (ps)
12 (no MCP)	1x	0.6	12	46	45
	3x	2.4	30	54	54
	10x	6.9	83	94	93
13 (MCP)	1x	0.6	13	46	43
	3x	2.4	33	55	58
	10x	6.9	90	100	101

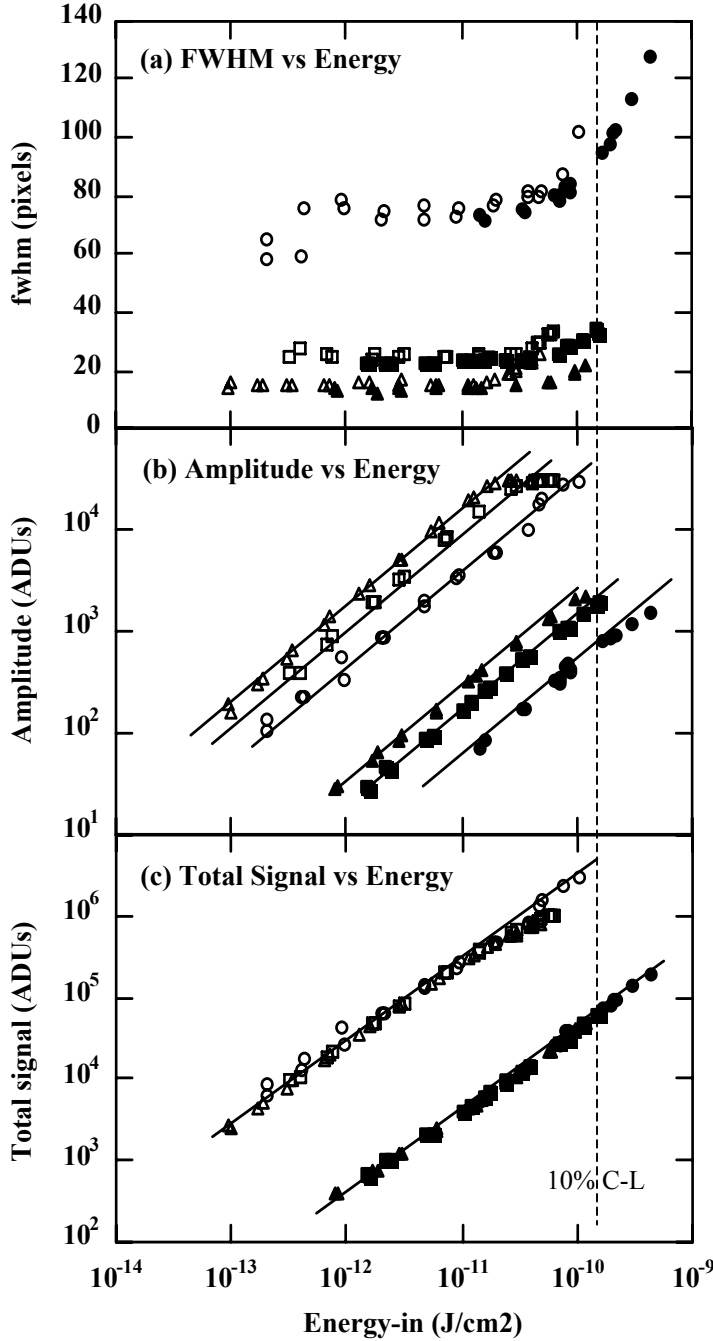
3.6 Dynamic Range

The concept of dynamic range is relatively simple: the maximum observable signal divided by the minimum observable signal. Unfortunately, problems quickly arise with the definitions used for the minimum and maximum observable signals. Are the signals quanta limited? Is the dynamic range quoted per CCD pixel, per CCD resolution element (2x2 pixel array), or camera resolution element (which depends on both spatial and temporal resolution). For this work, the dynamic range is presented per streak camera resolution element and per CCD resolution element.

The minimum signal S_{min} is conservatively taken as $5\sigma_{meas}$ per pixel as presented in Section 3.2. At this level, a signal will begin to rise above the background noise. Since dynamic range is calculated per resolution element for this article, the noise must be calculated per resolution element rather than per CCD pixel. If a resolution element contains N pixels, the noise sums across the pixels in the resolution element and minimum observable signal is given by $S_{min} = 5\sigma_{meas}N^{1/2}$. Thus for a 2x2 CCD limited resolution the minimum signal is given by $10\sigma_{meas}$.

The maximum signal S_{max} used for dynamic range calculations is somewhat more difficult to define. For this article, we use the signal at which the temporal pulse broadens by 20% independent of the broadening mechanism. A definition for the maximum signal based on temporal broadening depends on sweep speed and works best when the input pulse width is short relative to the streak camera resolution. When the streak tube is the limiting element, temporal broadening can be correlated with the C-L space-charge-limited current. A 20% broadening occurs at about 10 % of the C-L current.

To determine the maximum signals to be used for dynamic range calculations, temporal signals are recorded at various sweep speeds and signal amplitudes. For this work, 44-ps fwhm laser pulses were recorded with 1, 3, and 10-ns streak camera windows. Analysis typically uses three views of the data to help determine what actually limits the maximum signal: fwhm versus input energy, peak signal versus input energy, and total signal versus input energy. Data for the large-format CCD with and without a MCP IIT are shown in Fig. 8. With no IIT present, the large current density in the



streak tube needed to produce an output signal causes temporal broadening. A 20% broadening occurs at $\sim 10\%$ of the C-L space-charge-limited current. At all three sweep speeds the temporal signal broadens and the peak amplitude of the signal drops below a linear curve. But even so, the total integral of the signal remains linear with input signal indicating no loss of streak tube current.

Temporal broadening occurs at a lower signal intensity when the IIT is present. The peak current shows a sharp roll over at $\sim 32,000$ ADUs which is the maximum output of the CCD. The increase in temporal fwhm in this case occurs when the peak of the signal reaches CCD saturation. At this point, some of the signal is lost and the pulse area falls below the linear curve.

Once the 20% broadening point of the signal is found, then the maximum signal per CCD pixel can be calculated in either ADUs or photoelectrons. The maximum signal per resolution element is then N times this value. For high gain systems in which there are many ADUs per photoelectron, the minimum signal in a dynamic range calculation must be replaced by the equivalent signal of one photoelectron. This can be much greater than the system noise of $5\sigma_{\text{meas}}$.

4. DISCUSSION

Section 3 describes the basic characterizations that are used for evaluating streak camera performance. Characteristics for the three streak camera configurations examined in this study are presented in Table 4. The systems vary significantly in sensitivity from a low of 7.6 to a high of 2791 CCD electrons per

photocathode photoelectron, or equivalently 17.64 to 1193 ADUs per photoelectron. When sensitivity is compared to the measured noise level, configuration 2 is seen to be quanta limited. That is, a single photoelectron produces way more ADUs than the noise level (1193 to 28). For configuration 1, response to a single photoelectron is low relative to the noise level (17.6 to 28 ADUs).

Table 4. Summary of streak camera characterization results.			
Streak Camera Configuration	1. Large Format CCD, no IIT	2. Large Format CCD with IIT	3. Original Camera
RCA C73435 (S-20)	Yes	Yes	Yes
ITT F4113 MCP IIT	No	Yes	Yes
Photometrics SenSys 1600 CCD	No	No	Yes
SI S-800 CCD	Yes	Yes	No
System Sensitivity			
ADUs/pe ⁻	17.64	1193	25
CCD e ⁻ / pe ⁻	7.6	2791	500
Noise (3x3 binning)			
ADUs / pixel	28	28	1.4
Temporal resolution (ps)			
1 ns window	12	13	12
3 ns window	30	33	29
10 ns window	83	90	80
Spatial resolution			
LSF FWHM (μm)	50	~100	120
50% CTR (lp/mm)	7.5	2.2	3.8
5% CTR (lp/mm) limiting visual	20	9	9
Dynamic Range per resolution element / per CCD resolution element (4 pixels)			
Pixels	35 / 4	18 / 4	18 / 4
1 ns window	27 / 7	244 / 102	640 / 1563
3 ns window	86 / 29	163 / 102	640 / 1024
10 ns window	249 / 82	153 / 102	640 / 960

Temporal resolution is found to be independent of the streak camera configuration for all sweep speeds. Instead, temporal resolution depends primarily on the static line-width, sweep speed, and transit-time dispersion of the streak tube. There is no significant change in temporal resolution when the IIT is added or removed from the configuration. Resolution is dominated by the static line width and the dwell time.

There is, however, a significant improvement in the spatial resolution when the IIT is removed. The MCP IIT broadens the central LSF peak and increases the level of the wings relative to the central peak. Removal of the IIT clearly demonstrates the effect that the IIT veiling glare has on spatial resolution as all indicators improve (i.e. LSF width and CTR at 50 and 5%). When present, the MCP IIT limits the spatial resolution. This is why the two IIT configurations show the same spatial resolution.

The dynamic range varies considerably between the three camera configurations. Dynamic range results are reported per streak camera resolution element (spatial width times temporal width in pixels) and CCD resolution element (4 pixels) for each configuration at three different sweep windows. Configuration 1 without the IIT lacks enough amplification to clearly see a single photoelectron. This results in the low dynamic range values. An improvement in the relatively poor QE of 15% for this particular CCD to 75% would boost all the dynamic range values by a factor of 5. An additional factor of 2 in noise reduction would bring the total dynamic range improvement to a factor of 10. Configuration 2 has the opposite problem. The MCP IIT gain is too high which results in a very large signal for a single photoelectron. With the high gain, the system is linear until the CCD reaches its upper limit of 32,000 ADUs, but the minimum observable signal

of 1193 ADUs per photoelectron is well above the signal needed to simply surpass the noise. The large dynamic range that is associated with configuration 3 is simply a result of the camera optimization done in the late 1980s. Streak camera slit width, MCP gain matched to CCD coupling

ACKNOWLEDGMENT

This work was performed under the auspices of the U.S. Department of Energy by the University of California Lawrence Livermore National Laboratory under contract No. W-7405-Eng-48.

REFERENCES

1. LLNL high speed optical streak cameras
2. R. A. Lerche, "Timing between streak cameras with a precision of 10 ps," Proc. of SPIE Conference on Ultrahigh- and High-Speed Photography, Videography, Photonics, and Velocimetry '90, SPIE Vol. **1346**, pp. 376-383 (1990).
3. D. T. Attwood, R. L. Kauffman, G. L. Straddling, H. L. Medeck, R. A. Lerche, L. W. Coleman, E. L. Pierce, S. W. Thomas, D. E. Campbell, J. Noonan, G. R. Tripp, R. J. Schnetz, and G. E. Phillips, "Picosecond X-Ray Measurements from 100 eV to 30 keV", XIV International Congress on High Speed Photography and Photonics, (1980).
4. R. A. Lerche, D. W. Phillion, and G. W. Tietbohl, "Neutron detector for fusion reaction-rate measurements," Proc. of SPIE Conference on Ultrahigh- and High-Speed Photography, Videography, and Photonics, '93, SPIE Vol. **2002**, pp. 153-161 (1993).
5. J. D. Wiedwald and R. J. Hertel, "Veiling Glare in the ITT F4113 Image Intensifier", Proc. of SPIE Conference on High Speed Photography, Videography, and Photonics VI, SPIE Vol. **981**, pp. 154-160 (1988).
6. J. D. Wiedwald and R. A. Lerche, "Streak camera dynamic range optimization", Proc. of Conference on High Speed Photography, Videography, and Photonics V, SPIE Vol **832**, pp. 2275-282 (1987).
7. R. A. Lerche and R. L. Griffith, "Resolution limitations and optimization of the LLNL streak camera focus," Proc. of Conference on High Speed Photography, Videography, and Photonics V, SPIE Vol **832**, pp. 266-274 (1987).
8. R. Kalibjian and G. G. Peterson, "Analysis of space charge in photonic tubes", J. Appl. Phys., 54, pp. 4295-4301 (1983).